Permeation of Ethane through Polyethylene at Low Temperatures and Elevated Pressures

S. K. EVNOCHIDES
Monsanto Company, Texas City, Texas 77590

and ERNEST J. HENLEY
Chemical Engineering Department,
University of Houston, Houston, Texas 77004

Gas permeation through polymeric membranes is usually described in terms of an overall permeability coefficient which is defined as the steady state mass flux of gas per unit pressure difference across a membrane. This coefficient, however, provides only an overall description of the permeation process; a more fundamental formulation in terms of the solubility and diffusivity parameters is highly desirable. It was deemed important furthermore to obtain these parameters over a range of pressures and temperatures which encompass large deviations from ideal, fixed-gas behavior in order to achieve an explanation of several anomalous high-pressure, low-temperature effects which had previously been discovered (*1*). To achieve this purpose a direct reading, gravimetric sorption apparatus was employed.

Equilibrium Sorption in Polymers

The dissolution of penetrants by a solid polymer has been referred to as sorption in permeation literature, to include both adsorption and absorption mechanisms. For the system under consideration, absorption is considered the primary mechanism, the absorption taking place only in the amorphous regions (*2, 3*). The solubility isotherms are characteristic of what Rickles (*4*) calls a type IV system, the solubility being an exponential function of pressure [Equation (17)]. The parameter is, in a qualitative sense, related to the degree of polymer-penetrant interaction.

A number of statistical expressions based on various lattice theories for the polymer phase have been proposed and have met with some success. Among these are the original Flory-Huggins formulations (5, 6), which were later modified to account for free energy changes caused by elastic stretching (*7, 8*) and the presence of crystallites (*9*). Other approaches include Michael and Bixler's extension of the Jolley-Hildebrand treatment of gas solubility in liquids (*2*) and Stern, Mullhaupt, and Gareis' correlative-predictive technique based on the principle of corresponding states (*10*)

Diffusion in Polymers

Motion of penetrants through polymers presupposes two conditions: that the molecules possess adequate energy to overcome the potential barriers separating one position from another, and that the cooperative motion of the chain network continually create new vacancies of the proper size and shape. Pertinent theories include the transition state theory (*11*) and the activated zone theory of Barrer (*12*).

The glass transition point of the polymer has a profound effect on the diffusion characteristics. The activation energy for diffusion has been observed to decrease sharply in some systems (*13* to *16*) and time-dependent effects in glassy polymers have been observed (*17* to *20*). In the extreme, convective flow in addition to diffusion may occur. A mathematical treatment of combined flow has been given by Frisch (*21*).

The addition of plasticizers increases the diffusivity of a given gas or vapor through polymers (*22* to *25*). The presence of crystalline regions strongly decreases flow (*26, 27*).

EXPERIMENTAL EQUIPMENT AND PROCEDURES

Equipment

The arrangement of the experimental equipment is shown in Figure 1. The central piece of equipment was a Cahn RG Model Electrobalance mounted inside a high-pressure steel enclosure (the sorption cell). The polymer specimen is suspended directly from the balance beam with a 0.1-mm. diam. nickel-chrome wire. The electrobalance permits recording of weight changes with an ultimate sensitivity of 0.2 μg.

The sorption cell assembly is housed inside an insulated 36 in. × 48 in. × 30 in. thermostatically controlled wooden chamber. A ½-ton Tecumseh refrigeration system provided the cooling. Air bath temperature was controlled at ±2°F., but due to thermal lags, the cell temperature could be maintained to ±0.3°F.

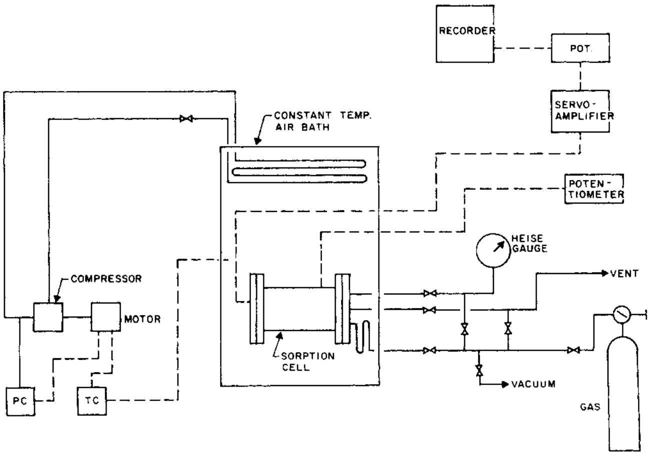

Fig. 1. Simplified diagram of sorption equipment.

Correspondence concerning this article should be addressed to Dean E. J. Henley.

Pressure measurements were made with a dead-weight calibrated, 12-in. Heise Model C precision gauge.

Auxiliary equipment included a Model G Leeds and Northrup recorder for monitoring the electrobalance signals, a Rubicon precision potentiometer for the iron-constantan thermocouples adjacent to the specimen, and a Duo-Seal Model 1402 Welch vacuum pump.

Procedures

1. The temperature is brought to the desired level. 2. The system is pressurized with gas to approximately 50 lb./sq. in. abs. and evacuated for at least 30 min. This is done a minimum of five times. 3. The polymer sample is conditioned at test temperature and pressure for 24 hr. 4. For the sorption experiments weight gains are recorded. These are corrected for buoyancy effects; the specific volume is calculated using the Benedict-Webb-Rubin equation of state. 5. The diffusion experiments are done by introducing step changes in pressure and recording weight changes as a function of time.

Materials

The membranes used were made from a commercially available low-density polyethylene manufactured by the Monsanto Company and marketed under the trade name MPE 72. The molded films were fabricated by the manufacturer in a platen press at a temperature of 320°F. and a pressure of 40,000 lb./sq. in. No antioxidants, plasticizers, or other additives were used. The following data were supplied by the manufacturer:

Polymer density: 0.9175 g./cc.
Number average molecular weight: 14,000
Weight average molecular weight: 351,000
Melt flow index (at 190°C.): 6.1
Intrinsic viscosity: 3.5
Amorphous fraction: 0.5215

The ethane was purchased from the Matheson Chemical Company in 225 cu. ft. cylinders. The gas was of C.P. grade and had a minimum purity of 99.5 mole %. The following analysis was provided by the supplier:

Component	Mole %
Ethane	99.3
Hydrogen	0.5
Methane	0.1
Ethylenes	0.1

THEORY

Diffusion

For unidirectional diffusion through a sheet of finite thickness $2L$, which is infinite in y and z, the diffusion equation is

$$\frac{\partial C}{\partial t} = \frac{\partial}{\partial x}\left(D(C) \frac{\partial C}{\partial x} \right) \tag{1}$$

In a transient state sorption experiment, a polymer membrane is initially placed in a gas atmosphere until a uniform gas concentration C_0 is established in the film. At time $t = 0$ the gas pressure is raised, the surface concentration of the permeant is changed to C_s, and sorption begins. With these boundary conditions Equation (1) can be solved if D is assumed to be independent of concentration.

When the solution, which is given by Crank (28), is integrated across the film thickness, we obtain an expression for the total mass of gas sorbed as a function of time:

$$\frac{M_t}{M_\infty} = 1 - \sum_{n=0}^{\infty} \frac{8}{(2n+1)^2 \pi^2} \exp\left[- \frac{D(2n+1)^2 \pi^2 t}{4L^2} \right] \tag{2}$$

Although integral diffusion coefficients can be obtained from Equation (2), it proved convenient to use a solution for very short times, that is, before the centerline concentration has changed. With the boundary conditions

$$\begin{array}{lll} C = C_0 & x > 0 & t = 0 \\ C = C_s & x = 0 & t > 0 \\ C = \text{Finite} & x = \infty & \end{array} \tag{3}$$

the solution of Equation (1) becomes

$$\overline{C} = 1 - \operatorname{erf} \frac{x}{2\sqrt{Dt}} \tag{4}$$

where

$$\overline{C} = \frac{C - C_0}{C_s - C_0}$$

Integration of Equation (4) to give an expression for the fractional mass gain gives

$$\frac{M_t}{M_\infty} = \frac{2}{\sqrt{\pi}} \left[\frac{Dt}{L^2} \right]^{1/2} \tag{5}$$

The diffusion coefficient can be conveniently calculated from the initial slope R of the M_t/M_∞ versus $t^{1/2}$ curve according to

$$D = \frac{\pi}{4} L^2 R^2 \tag{6}$$

When the diffusion coefficient is a function of concentration, Equation (1) has no general solution, although approximate solutions to special cases can be achieved (29, 30). If one applies the Boltzmann transformation [Equation (7)], Equation (1) for short times is reduced to an ordinary differential equation, Equation (8):

$$\eta = \frac{1}{2} \frac{x}{\sqrt{D_0 t}} \tag{7}$$

$$-2\,\eta \frac{d\overline{C}}{d\eta} = \frac{d}{d\eta}\left(\frac{D}{D_0} \frac{d\overline{C}}{d\eta} \right) \tag{8}$$

where D_0 is the diffusivity at a concentration C_0. Applying the boundary conditions of Equation (3)

$$\begin{array}{ll} \overline{C} = 0 & \eta = \infty \\ \overline{C} = 1 & \eta = 0 \end{array} \tag{9}$$

and integrating twice we arrive at

$$\overline{C} = 1 - \frac{\int_0^{\eta} \frac{1}{D/D_0} \exp\left[- \int_0^{\eta} \frac{2\eta}{D/D_0}\, d\eta \right] d\eta}{\int_0^{\infty} \frac{1}{D/D_0} \exp\left[- \int_0^{\eta} \frac{2\eta}{D/D_0}\, d\eta \right] d\eta} \tag{10}$$

Equation (10) reduces to Equation (4) when D equals D_0. In terms of the measured variable, the fractional weight gain is given by

$$\frac{M_t}{M_\infty} = \frac{2(D_0 t)^{1/2}}{L} \int_0^{\infty} \overline{C}\, d\eta \tag{11}$$

Permeability

Both the solubility and the diffusivity affect the permeability, which is defined as the steady state flux of penetrant per unit pressure difference across the membrane

$$\mathbb{P} = \frac{JL_f}{\Delta P} \tag{12}$$

At steady state, and assuming concentration-independent diffusion, Equation (1) can be integrated to yield

$$-D\frac{dC}{dx} = J = \text{constant} \qquad (13)$$

Integrating again between $x = 0$ (where $C = C_1$) and $L = L_f$ (where $C = C_2$)

$$J = \frac{1}{L_f}\int_{C_2}^{C_1} D \qquad (14)$$

The ideal permeability case arises when the solubility of the gas in the polymer follows Henry's law, and the diffusion coefficient is constant. Then Equations (14) and (12) can be combined and integrated to yield

$$|\mathrm{P} = D \cdot K \qquad (15)$$

For all other cases $|\mathrm{P}$ can be obtained by integration of Equation (16) if the solubility-pressure relationship and the concentration dependency of the diffusivity are known:

$$|\mathrm{P} = \frac{1}{P_1 - P_2}\int_{C_2}^{C_1} D\, dC \qquad (16)$$

TABLE 1. RESULTS OF SOLUBILITY EXPERIMENTS

Temperature, °F.	Pressure range, lb./sq.in.abs.	δ	$S_0 \left(\frac{g}{g}\right)$	No. of experiments
76	30 to 300	0.00006	0.001092	21
51	19 to 268	0.01242	0.001337	21
48.4	15 to 265	0.01375	0.001337	21
38.9	19 to 262	0.04018	0.001479	18
29.1	19.5 to 260	0.10032	0.001558	17
17.9	16.2 to 263	0.11738	0.001720	13
7.9	15.6 to 232	0.13920	0.001894	12
−1.0	22.5 to 210	0.14411	0.002136	14
−15.0	25.1 to 168	0.15780	0.002410	14

TABLE 2. RESULTS OF SORPTION EXPERIMENTS

Temperature, °F.	P_o, lb./sq.in.abs.	P_s, lb./sq.in.abs.	$\overline{D}$, sq.cm./sec., 10^7	C_s, g./g.
76.10	16.7	40.2	0.7583	0.002987
76.10	40.2	80.3	0.9711	0.005967
76.10	80.3	118.2	1.213	0.008783
76.10	118.2	158.6	1.576	0.01179
76.10	158.6	199.2	1.962	0.01480
76.10	199.2	253.9	2.849	0.01887
38.90	15.5	38.5	0.1593	0.003879
38.90	38.5	76.6	0.2272	0.007768
38.90	76.6	114.6	0.3423	0.01167
38.90	114.6	158.6	0.5023	0.01622
38.90	158.6	198.4	0.7369	0.02038
38.90	198.4	253.0	1.156	0.02614
7.80	15.8	38.1	0.02991	0.005018
7.80	38.1	77.0	0.0524	0.01037
7.80	77.0	115.8	0.1021	0.01594
7.80	115.8	15.8	0.2064	0.0228
7.80	158.0	197.1	0.3943	0.02842
7.80	197.1	236.9	0.7416	0.03494
−0.90	16.0	40.0	0.01937	0.005971
−0.90	40.0	77.6	0.03530	0.01188
−0.90	77.6	115.2	0.08446	0.01808
−0.90	115.2	155.5	0.1771	0.02570
−0.90	155.5	208.5	0.5362	0.03482
−15.0	15.1	32.1	0.01044	0.005419
−15.0	32.1	68.1	0.02123	0.01188
−15.0	68.1	102.9	0.05004	0.01853
−15.0	102.9	129.5	0.1129	0.02389
−15.0	129.5	164.2	0.2783	0.03127

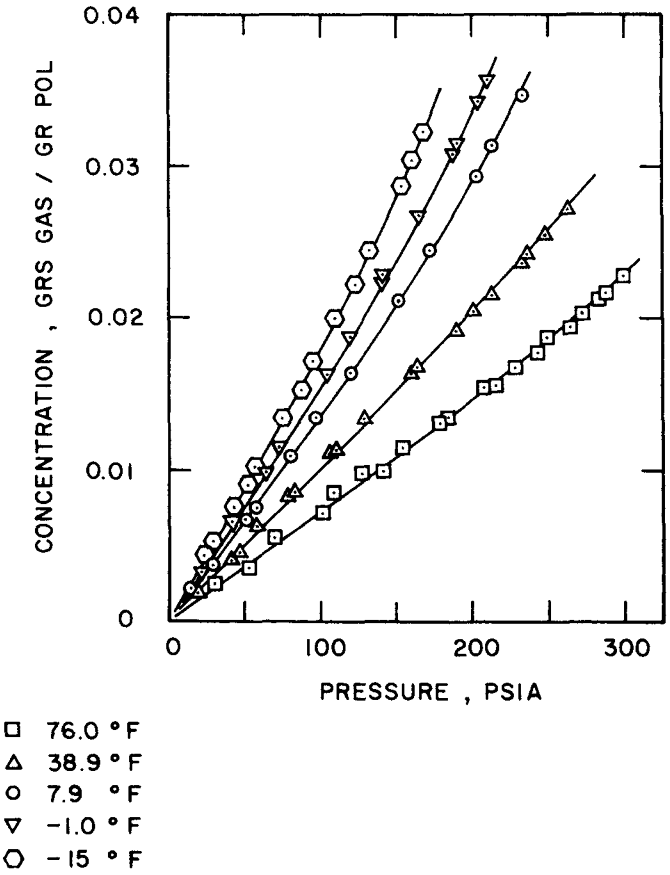

Fig. 2. Sorption isotherms systems; ethane-polyethylene.

EXPERIMENTAL RESULTS AND DISCUSSION

Equilibrium Solubilities

As can be seen from Figure 2, there is a nonlinear relationship between concentration and pressure. The pressure dependence of the solubility coefficient $S = C/P$ is represented by the expression

$$S = S_0 \exp\,(\delta\ P/P^0) \qquad (17)$$

where P^0 is the vapor pressure of ethane at the isotherm temperature, S_0 the solubility coefficient at $P = 0$ and δ the parameter characteristic of the deviation from Henry's law behavior. Values of δ obtained by a nonlinear least squares regression analysis are given in Table 1.

The amorphous fraction of the film, as calculated by the method of Michaels and Bixler (*2*), is 0.5215. Using this value, the corrected solubility at 1 atm., 1.43 cc. (*STP*)/cc. amorphous polymer, is in excellent agreement with that report by Michaels and Bixler [1.35 cc. (*STP*)/cc. amorphous polymer].

To obtain an estimate of the precision of the measurements, a number of observations were made at 75°F. and at 30 lb./sq.in.abs., this pressure being approached in both directions. Assuming the error to be normally distributed, we found the relative error at the 95% confidence level to be ±3%. This corresponds to a maximum relative error for the solubility of 4%, with somewhat lower figure at the higher pressures. No hysteresis effects were observed.

The parameters S_0 and δ listed in Table 1 were obtained using the Marquardt nonlinear least square fit, the program being given by Henley and Rosen (*31*). The 95% confi-

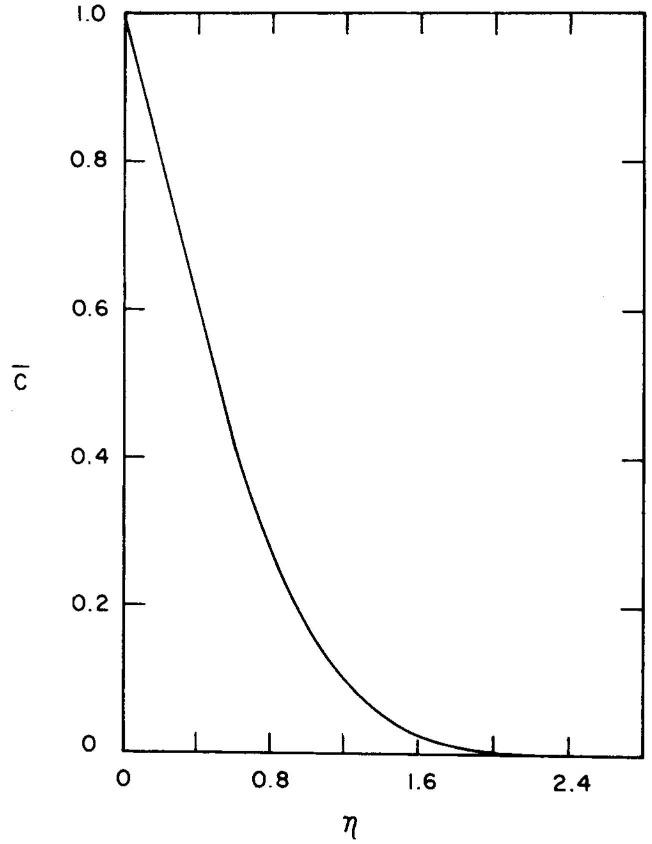

Fig. 3. Integral diffusion coefficients; curves computed using $D < D_0 \exp(\alpha C)$.

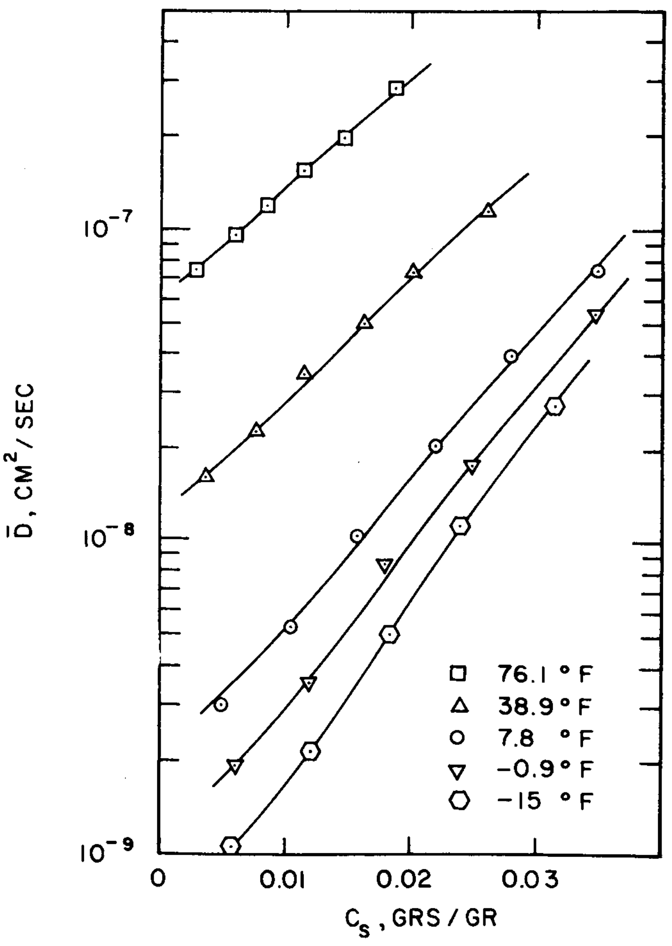

Fig. 4. Concentration profile for run 1204-1.

dence contour for these parameters for a typical isotherm was determined according to the method of Draper (*32*).

Sorption Studies

Transient state sorption experiments were made at 76° to −15°F. at pressures between 15.5 and 253 lb./sq.in.abs. An integral diffusion coefficient $\overline{D}$ in the interval ($P_0 - P_s$) as calculated by Equation (6) is given in column 4 of Table 2 and in Figure 3. The experiments were done successively, that is, the P_s from the last run became P_0 for the succeeding run.

Point diffusion coefficients D were obtained by an iterative trial and error process. The method is a modification of a procedure originally proposed by Crank (*28*), and uses the following approximation for obtaining successive estimates of D as a function of concentration:

$$\overline{D}_i \cong \frac{1}{C_i - C_{i-1}} \int_{C_{i-1}}^{C_i} D\, dC \qquad (18)$$

1. The integral diffusion coefficient D_i is calculated from the initial slope, for each pressure interval, via Equation (6).

2. For each C_i Equation (18) is used to calculate the quantity I_i for $i = 1, 2 \ldots m$

$$I_i = \int_{C_0}^{C_i} D\, dC = \sum_{j=1}^{j=i} \overline{D}_j\, (C_j - C_{j-1}) \qquad (19)$$

In Equation (19) C_0 is the initial concentration for the first sorption interval and m is the total number of sorption intervals.

3. A polynomial curve fit of the quantity I_i as a function of C_i is made, and a first estimate of the point diffusion coefficient D is obtained by numerical differentiation, that is

$$D_{C=C_i} = \left[\frac{d}{dC} \int_{C_0}^{C} D dC \right]_{C=C_i} \qquad (20)$$

This produces a curve of D versus C.

4. An initial estimate of the concentration distribution is made by substituting various values of η into Equation (4).

5. Values of $D(\eta)$ are obtained for each calculated $\overline{C}$ using the curve of D versus C obtained in step 3.

6. The $D - \eta$ values are used to obtain values for $\overline{C}$ via Equation (10).

7. Values of $\overline{C}$ calculated in step 6 are compared to those estimated in step 4. If these values disagree, the step 6 $\overline{C}$'s are used to obtain new $D(\eta)$'s and the procedure is repeated until a concentration profile consistent with the D's obtained in step 3 are obtained. The final profile must satisfy the conditions

$$\left[\frac{D}{D_0} \frac{d\overline{C}}{d\eta} \right]_{\eta=0} + 2 \int_0^\infty \overline{C} d\eta = 0 \qquad (21)$$

A typical curve is shown in Figure 4.

8. Equation (1) is used to obtain an expression for M_t/M as a function of t. The upper limit on η is set sufficiently high for $\overline{C} \cong 0$. The initial slopes of the curve are used to obtain $\overline{D}_i$ as in 1.

Steps 4 to 8 are repeated for each interval.

9. The $\overline{D}_i$'s from step 8 are compared to the experimental values from step 1. If satisfactory agreement has been obtained, the calculation is terminated; if not, we obtain new D_i's using the calculated $\overline{C}$'s via steps 2 and 3

and iterate.

In general, the inner loop of Figure 5 converged after three to five iterations, and the outer loop after two to three.

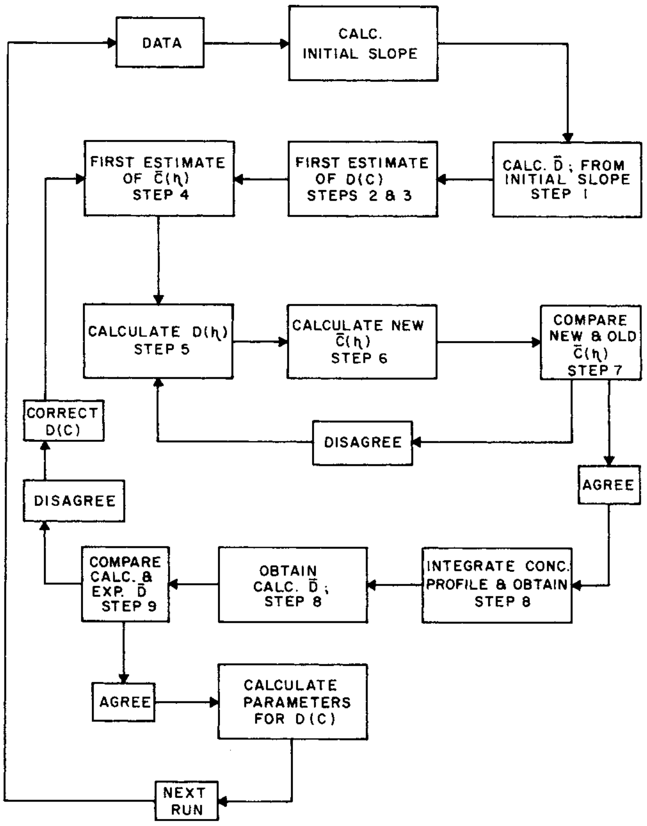

Fig. 5. Simplified block diagram for calculation of $D(C)$.

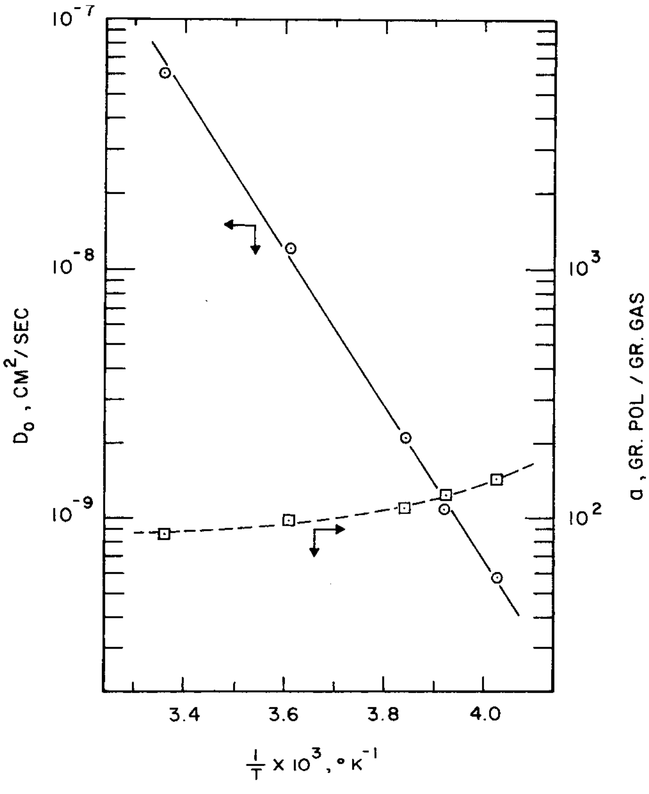

Fig. 6. Effect of temperature on D_0 and a.

Based on replication experiments, the relative error in determining D was estimated as ±5% at the 95% confidence level.

The Effect of Temperature on *D*

When the diffusion coefficients of the ethane-polyethylene system are plotted as a function of concentration on semilogarithmic paper, a straight line is obtained, suggesting a relationship of the form

$$D = D_0 \exp(\alpha C) \tag{22}$$

D_0, the limiting diffusion coefficient at zero penetrant concentration, decreases rapidly with decreasing temperature and follows an Arrhenius relationship (Figure 6):

$$D_0 = D_0' \exp(-E_{D0}/RT) \tag{23}$$

In addition to the kinetic effects of temperature, the energy of activation also reflects changes in the morphology of the polymer. Increased crystallinity at lower temperatures would be expected to decrease D in three ways: by decreasing the available volume for diffusion, by increasing the tortuosity in bypassing crystallites, and by decreasing the mobility of the amorphous chain segments as a result of the crosslinking action of the crystallites.

The value of α, on the other hand, increases as the temperature is decreased. This parameter is a measure of the loosening of the polymer structure due to the presence of penetrant which causes a substitution of polymer-polymer contacts with polymer-penetrant contacts. At relatively high temperatures the internal mobility of the chains and chain segments is quite high, and the presence of the penetrant produces a relatively obscure effect. As the temperature is lowered near the vicinity of the glass transition point, chain mobility is reduced drastically and the presence of the penetrant has a much more pronounced plasticizing influence.

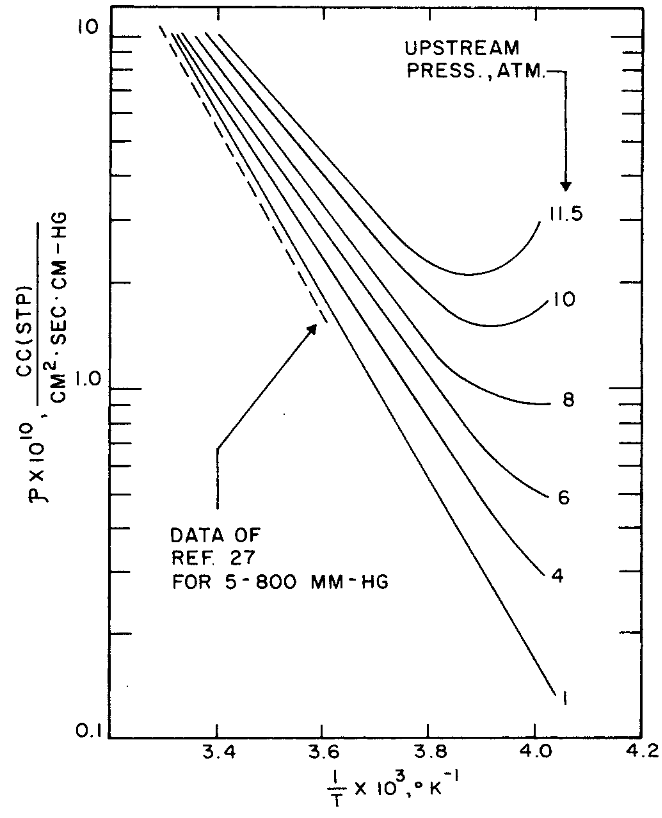

Fig. 7. Computed permeability isobars system ethane-polyethylene; downstream pressure, 0.001 atm.

Permeabilities

Combining Equations (16), (17), and (22) and integrating, we obtain

$$\mathbb{P} = \frac{D_0}{(P_1 - P_2)} \exp\left[\alpha\, S_0 P_1 \exp\left(\frac{\delta}{P^0} P_1 \right) \right] - \exp\left[\alpha\, S_0 P_2 \exp\left(\frac{\delta}{P^0} P_2 \right) \right] \qquad (24)$$

where subscripts 1 and 2 refer to the upstream and downstream sides of the film, respectively. For $\delta = \alpha = 0$, Equation (24) reduces to Equation (15).

Equation (24) was used to compute permeabilities for the ethane-polyethylene system as a function of temperature and upstream pressure. The results are shown graphically in Figure 7 at a low (0.001 atm.) reference pressure. As expected, the permeabilities depend very strongly on pressure, especially at the lower temperatures where the deviations from ideality are large. The pressure dependence is much less pronounced at the higher temperatures. As the temperature is reduced, the mobility of the polymer chains and chain segments is decreased and, at low pressures, a reduction in the permeability coefficients is observed. However, at sufficiently high pressures the increased concentration of dissolved penetrant creates sufficient plasticization to overcome the temperature effect, and a minimum in the permeability versus $1/T$ curve is obtained. Further reduction in temperature results in an increase in permeability due to overcompensation of the temperature effect. The minimum temperature increases as would be expected, with increasing pressure.

Roberts et al. (*33*) observed a similar behavior of measured permeabilities for methyl bromide in polyethylene. Similarly, the permeability data of Henley and Santos (*1*) for ethane-polyethylene showed a minimum at approximately the same temperatures. However, their permeability values are considerably higher than those computed in this work. Differences in polymer crystallinity and branching could account for at least part of this discrepancy. Another comparison with experimentally determined permeabilities can be made with the data of Michaels and Bixler (*26*), who measured permeation rates of ethane through a polyethylene of similar crystallinity. Michaels and Bixler did not observe a pressure dependence of permeabilities over the range of temperatures (5° to 50°C.) and pressures (5 to 800 mm. Hg) covered in their work. However, their results are in excellent agreement with their computed values for these conditions (Figure 7).

NOTATION

C = concentration of penetrant in polymer, g. penetrant/g. polymer
C_0 = concentration of penetrant at $t = 0$
C_s = surface concentration
$\overline{C}$ = dimensionless concentration as defined by Equation (4)
D = diffusion coefficient, sq.cm./sec.
$\overline{D}$ = integral diffusion coefficient, Equation (18)
D_0 = diffusion coefficient at zero concentration, sq.cm./sec.
D_0' = pre-exponential factor for Arrhenius relationship of diffusion coefficient
E_{D_0} = activation energy for diffusion, cal./g.-mole
I = parameter in Equation (19)
J = mass flux, g./(sec.)(sq.cm.)
$\overline{K}$ = Henry's law constant, g. gas/(g. polymer)(atm.)
$\overline{L}$ = half-thickness of polymer membrane
L_f = thickness of polymer film
M_t = amount of gas sorbed at time t, consistent units
M_∞ = amount of gas sorbed at equilibrium, consistent units
P^0 = vapor pressure, consistent units
$\mathbb{P}$ = permeability coefficient, cc.(STP)/(cm.)(sec.)(cm. Hg)
R = initial slope, Equation (6)
R = gas constant, consistent units
S = solubility of penetrant in polymer, g. penetrant/(g. polymer)(atm.)
t = time, sec.
T = temperature, °K.
x = direction in which mass is diffusing across a thin flat sheet
α = parameter in the diffusivity Equation (22)
η = $x/\sqrt{4D_0t}$
δ = solubility parameter as defined by Equation (17), dimensionless

LITERATURE CITED

1. Henley, E. J., and M. L. D. Santos, *AIChE J.*, **13**, 1119 (1967).
2. Michaels, A. S., and H. J. Bixler, *J. Polymer Sci.*, **50**, 393 (1961).
3. Sobolev, J., J. A. Mayer, V. Stannett and M. Szwarc, *Ind. Eng. Chem.*, **49**, 441 (1957).
4. Rickles, R. N., *ibid.*, **58** (6) (1966).
5. Flory, P. J., *J. Chem. Phys.*, **10**, 51 (1942).
6. Huggins, M., *ibid.*, **9**, 440 (1941).
7. Flory, P. J., and J. Rehner, *ibid.*, **12**, 412 (1944).
8. Kumins, C. A., and J. Roteman, *J. Polymer Sci.*, **A1-1**, 541 (1963).
9. Rogers, C. E., V. Stannett, and M. Szwarc, *J. Phys. Chem.*, **63**, 1406 (1959).
10. Stern, S. A., J. T. Mullhaupt, and P. J. Gareis, *AIChE J.*, **15**, 1, 64 (1969).
11. Glasstone, S., K. J. Laidler, and H. Eyring, "The Theory of Rate Processes," McGraw-Hill, New York (1941).
12. Barrer, R. M., "Diffusion in and Through Solids," Cambridge Univ. Press, Cambridge (1951).
13. Bagley, E., and F. A. Long, *J. Am. Chem. Soc.*, **77**, 2172 (1955).
14. Barrer, R. M., J. A. Barrie, and J. Slater, *J. Polymer Sci.*, **27**, 177 (1958).
15. Meares, P., *Trans. Faraday Soc.*, **53**, 1148 (1957).
16. Van Amerongen, G. J., *J. Polymer Sci.*, **5** (3), 307 (1950).
17. Meares, P., *Trans. Faraday Soc.*, **54**, 41 (1958).
18. Newns, A. C., *ibid.*, **52**, 1533 (1956).
19. Rosen, B., *J. Polymer Sci.*, **47**, 19 (1960).
20. *Ibid.*, **49**, 177 (1961).
21. Frisch, H. L., *J. Phys. Chem.*, **60**, 1177 (1956).
22. Brubaker, D. W., and K. Kammermeyer, *Ind. Eng. Chem.*, **44**, 1465 (1952).
23. *Ibid.*, **45**, 1148 (1953).
24. Heilman, W., V. Tamella, J. A. Meyer, V. Stannett, and M. Szwarc, *ibid.*, **48**, 821 (1956).
25. Kumins, C. A., C. J. Rolle, and J. Roteman, *J. Phys. Chem.*, **61**, 1290 (1957).
26. Michaels, A. S., and H. J. Bixler, *J. Polymer Sci.*, **50**, 413 (1961).
27. Michaels, A. S., and R. B. Parker, *ibid.*, **41**, 53 (1959).
28. Crank, J., "The Mathematics of Diffusion," Oxford Univ. Press, London (1956).
29. Fujita, H., *Text. Res. J.*, **22**, 757 (1952).
30. *Ibid.*, 823 (1952).
31. Henley, E. J., and E. M. Rosen, "Materials and Energy Balance Computations," Wiley, New York (1969).
32. Drayer, N. R., and H. Smith, "Applied Regression Analysis," Wiley, New York (1967).
33. Rogers, C. E., V. Stannett, and M. Szwarc, *TAPPI*, **44** (10), 715 (1961).

Manuscript received January 20, 1970; revision received May 22, 1970; paper accepted May 28, 1970.